2017

# Analysis and Design of a Highly Compact Ellipse-Shaped Ultra-Wideband Bandpass Filter (Uwb-Bpf) with a Notched Band

Xuetan Liu
*University of South Carolina*

# ANALYSIS AND DESIGN OF A HIGHLY COMPACT ELLIPSE-SHAPED ULTRA-WIDEBAND BANDPASS FILTER (UWB-BPF) WITH A NOTCHED BAND

by

Xuetan Liu

Bachelor of Science
The Ohio State University, 2014

---

Submitted in Partial Fulfillment of the Requirements

For the Degree of Master of Science in

Electrical Engineering

College of Engineering and Computing

University of South Carolina

2017

Accepted by:

Yinchao Chen, Director of Thesis

Md Moinul Islam, Reader

Cheryl L. Addy, Vice Provost and Dean of the Graduate School

# DEDICATION

To my family, who has always been there to support me along the way for me to achieve my academic objectives.

To Dr. Yinchao Chen, who has been patient to guide me working through all technical issues during the proposed research and design.

# ACKNOWLEDGEMENTS

I would like to acknowledge my major professor, advisor and committee chair Dr. Yinchao Chen. He is very knowledgeable and professional in electromagnetic fields and communication and he is always really patient and supportive when some issues were encountered. All the feedbacks and responses from him in the past two years are really impactful and helpful, which is a very important factor leading to success of this thesis.

I would also like to acknowledge my advisory committee member Dr. Md Moinul Islam who is always supportive, not only to my academic work, but also to my course work and personal sphere.

By this opportunity, I would like to specially thank Mr. Dave London, Ms. Nat Paterson and Ms. Jenny Balestrero for helping me solve technical problems occurred in the past two years. Also, thanks to Lab of Signal Integrity of Department of Electrical Engineering, University of South Carolina for providing a great working environment and all useful software including HFSS and ADS.

In addition, all other supports from department officers and other colleagues are highly acknowledged.

# ABSTRACT

Since the Federal Communications Commission's endorsement of the frequency band of 3.1 – 10.6 GHz in 2002 to be unlicensed for wireless communication applications, various ultra-wideband bandpass filters (UWB-BPFs) have been proposed and designed. Different UWB-BPF configurations were presented in the past years to meet the very strict UWB-BPF specifications in terms of ultra-band requirement, low return loss, high rejection in notched bands. However, most of the previous works are limited by large dimension size, complex geometry, and high production cost.

The major objective of this work is to design a highly compact, simple geometry, and low-cost UWB-BPF, which passes signals in nearly all frequencies in the passband with minimum loss but rejects unwanted WLAN interference signals in the frequency neighborhood of 5.8 GHz. First, an ellipse-shaped UWB-BPF was designed by using a simplified composite right/left handed (SCRLH) resonator to achieve a 3dB bandwidth ranging from 2.94 GHz to 12.83 GHz. Then, two open, curved stepped-impedance stubs were integrated into the UWB-BPF to achieve a notched band in the range of 5.8 GHz, such that the frequency response in the frequency band was sharply notched up to about 35dB attenuation. The finalized UWB-BPF, is simply built up with a commonly used PCB with FR4 substrate and has a dimension of 14mm × 6.2mm. The extracted current density images in the passbands, stop bands, and notch band clearly demonstrate the mechanism of the signal response characteristics of the proposed UWB-BPF.

# TABLE OF CONTENTS

# LIST OF TABLES

# LIST OF FIGURES

# LIST OF SYMBOLS

| | |
|---|---|
| $F_L$ | Lower cut-off frequency of a bandpass filter |
| $F_H$ | Higher cut-off frequency of a bandpass filter |
| $R$ | Resistance |
| $C$ | Capacitance |
| $F_r$ | Resonant frequency |
| $L_L$ | Shunt inductance |
| $L_R$ | Series inductance |
| $C_R$ | Shunt capacitance |
| $C_L$ | Series capacitance |
| $\beta$ | Propagation constant for Bloch waves |
| ZB | Characteristic impedance of the unit cell of SCRLH resonator |
| d | Length of the unit cell of SCRLH resonator |
| $Q$ | Quality factor |
| $F_N$ | Notch frequency |
| $L$ | Left-handed shunt inductance measured at two vias |
| $L_{R1}$ | Right-handed series inductance induced by the ellipse-shaped ring |
| $C_1$ | Right-handed shunt capacitance induced by the ellipse-shaped ring |
| $L_{R2}$ | Inductance affected by the cross-shaped microstrip line segments |
| $Z_0$ | Characteristic impedances of the matched input and output lines of the SCRLH resonator |

$Z_1$ Characteristic impedance of the left SI stub

$Z_2$ Characteristic impedance of the right SI stub

$\Theta_0$ Electrical length of $Z_0$

$\Theta_1$ Electrical length of $Z_1$

$\Theta_2$ Electrical length of $Z_2$

$Y_1$ Admittance of the left SI stub

$Y_2$ Admittance of the right SI stub

$d\varphi$ Phase change

$d\omega$ Frequency change

# LIST OF ABBREVIATIONS

ADS ……Advanced Design System

BPF …….....Bandpass Filter

CRLH ……...Composite Right/Left Handed

DGS……...Defected Ground Structure

FCC……..Federal Communications Commission

HFSS ……High Frequency Electromagnetic Field Simulation

PCB …….Printed Circuit Board

RF …….....Radio Frequency

SCRLH……...Simplified Composite Right/Left Handed

SI…….....Stepped-Impedance

SW-HMSIW……Slow-wave Half-Mode Substrate-integrated Waveguide

TL……..Transmission Line

UWB……...Ultra-wideband

WLAN……...Wireless LAN

# CHAPTER 1 INTRODUCTION

## 1.1 Introduction

The unlicensed frequency band application in the range of 3.1 through 10.6 GHz approved by the U.S Federal Communications Commission (FCC) in early 2002 has strongly stimulated great growth, expansion and exploration of ultra-wideband (UWB) technology for different commercial and personal wireless communication applications [1]. Correspondingly, the ultra-wideband bandpass filters (UWB-BPFs) has been highly demanded in the development of various modern UWB communication systems, especially for those requiring the characteristics of sharp selectivity and capabilities to avoid interference from existing radio signals.

There has been increasing research since then in the area of UWB-BPF design with or without notched bands for various UWB applications. In 2007, Shaman and Hong firstly designed a UWB-BPF with embedded band notch structures as published in [1]. Wong and Zhu designed a compact UWB-BPF implemented with a notched band in the following year [2]. The stepped-impedance stubs in a ring resonator were designed by Kim and Chang in [3] to achieve the switchable bandwidth for a bandpass filter. In 2009, Hao and Hong designed a UWB-BPF with short-circuited stub resonators in a nonuniform multilayer periodical structure [4].

To abandon unwanted interference signals from WLAN applications, a multiple band UWB-BPF is preferred based on practical circumstances [5-21]. There are many published designs that can achieve a UWB passband with single or multiple notched bands. For example, in [9], a short-circuited L-shaped resonator was added to a UWB-BPF for offering a notched band by using a slow-wave half-mode substrate-integrated waveguide (SW-HMSIW). However, it required a complicated geometry configuration and had low rejection in its notched band. In [8], a pair of cross-shaped microstrip line segments is used to achieve a UWB-BPF, but the dimension size of the designed structure can be certainly improved as discussed in this work.

## 1.2 Objectives of the Research

This research will focus on design, improvement, and development of a UWB-BPF for potential UWB system applications based on previously published works [5-21]. Thus, the objective of this work is to propose a novel UWB-BPF characterized as follows:

- Maximize the UWB-BPF pass bandwidth to meet the system requirements in sharp selectivity and high capability;
- Highly reject unwanted WLAN interference signals in the frequency range of 5.8 GHz and ensure high quality of received signals;
- Minimize the UWB-BPF dimensions and keep it low profile such that it can be potentially applied in most UWB systems;

- Simplify the UWB-BPF geometry while remaining high performance for both its return loss and insertion loss so that the design and fabrication cycle can be much shortened;
- Reduce the cost of UWB-BPF production by using commonly used PCBs.

In this work, a new ellipse-shaped UWB-BPF will be designed with a coupled simplified composite right/left handed (SCRLH) resonator and two open stepped-impedance (SI) stubs to meet all the requirements as described above.

## 1.3 Content of the Thesis

There will be six chapters in this thesis. The first chapter is Introduction to this thesis, which states and summarizes the previously published works, project objectives, and overview of the thesis. The second chapter of this thesis mainly discusses the background and concepts used in the UWB-BPF analysis and design. Chapter 3 presents a detail design of simplified composite right/left handed (SCRLH) UWB-BPF, displays characteristics of S-parameters for the proposed UWB-BPF, and discusses possible potential issues for the current version of this design. Consequently, chapter 4 focuses on development and enhancement of the UWB-BPF developed in chapter 3 by inserting a notched band to the designed passband. In chapter 5, the designed system is modeled and validated in High Frequency Electromagnetic Field Simulation (HFSS). The proposed UWB-BPF was compared to those recently published and comparison and analysis were presented at the end of this chapter. Finally, chapter 6, the last chapter of this thesis,

concludes the research and suggests some future work for the extended UWB-BPF analysis and design.

# CHAPTER 2 BACKGROUND AND CONCEPTS USED IN UWB-BPF DESIGN

This chapter will mainly focus on introduction and discussion of the technical background and basic concepts related to UWB-BPF analysis and design. Especially, the characteristics and terminologies of BPF, UWB-BPF, SCRLH resonator, band-stop filter and notch filter will be briefly discussed in this chapter.

## 2.1 Bandpass Filter (BPF)

A bandpass filter (BPF) passes signals within a certain range of frequencies without much distorting input signals or introducing extra noise. This range of frequencies is commonly known as the filter bandwidth [22].

Bandwidth represents the frequency range between the lower cut-off frequency ($f_L$) and the higher cut-off frequency ($f_H$) points as defined in (2.1) or Figure 2.1:

$$Bandwidth = f_H - f_L \tag{2.1}$$

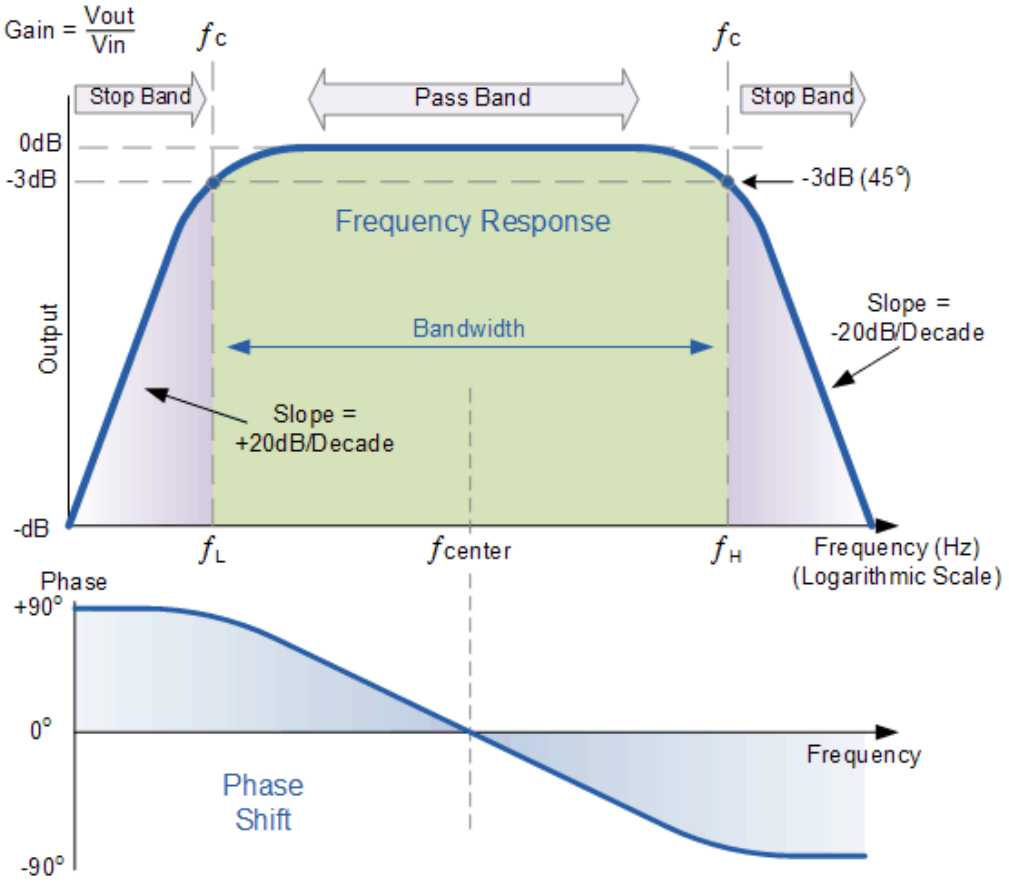


Figure 2.1 Typical frequency response for a bandpass filter [22].

When the output gain reaches its maximum value, the frequency on that point is known as the resonant frequency ($f_r$). It is simply the geometric average that can be evaluated as follows [22]:

$$f_r = \sqrt{f_L \times f_H} \qquad (2.2)$$

where $f_r$ is the resonant frequency, $f_L$ and $f_H$ are, respectively, the lower -3dB cut-off frequency and upper -3dB cut-off frequency [22].

## 2.2 Band-Stop Filter and Notch Filter

Band-stop filter passes all frequencies except for those within a specific stop band, and it is expected that signals are highly attenuated in the stop band. Similar to a band pass filter, the bandwidth and two cut-off frequencies for a stop band are defined as the stop band bounded by the two edge frequency -3dB points or cut-off frequencies as shown in Figure 2.2.

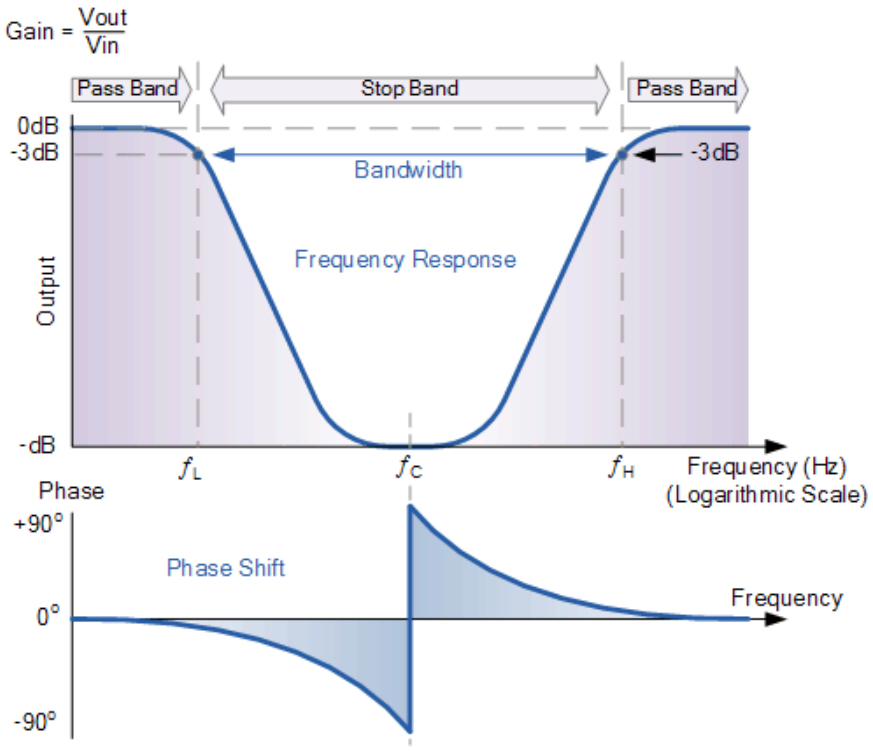


Figure 2.2 Frequency response for a band-stop filter [23].

Notch filter is a band-stop filter with a narrow stopband and a high Q factor. It passes most frequencies but attenuates a specifically small range of frequencies to very low levels and its frequency response usually by design shows a deep notch with high

selectivity. For example, a commonly used notch filter is the twin-T notch filter network shown in Figure 2.3 [23].

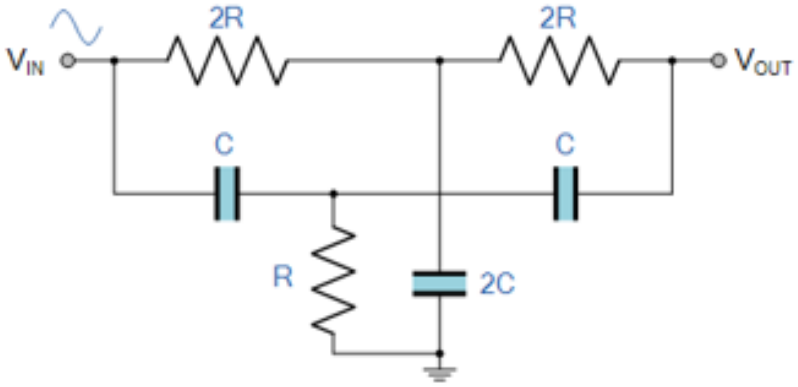


Figure 2.3 Schematic circuit of a basic twin-T notch filter [23].

The notch frequency $f_N$ at which the basic twin-T notch filter achieves maximum attenuation is calculated by the formula below [23]:

$$f_N = \frac{1}{4\pi RC} \tag{2.3}$$

where R and C are defined in Figure 2.3.

There are many applications of band-stop or notch filters in communication circuits, because they can be used to block a band of unwanted frequency signals from a system while allowing passband frequency signals to enter with minimum loss.

## 2.3 Ultra-wideband Bandpass Filter (UWB-BPF)

Ultra-wideband (UWB) technology is specially referred as a “radio technology that uses a very low energy level for short-range, high-bandwidth communications over a large portion of the radio spectrum”, which was pioneered by Robert A. Schorton in his work published in 2004 [28]. The bandwidth of UWB emitted signal needs to be at least 500 MHz [28].

In 2002, FCC authorized the unlicensed use of UWB in the frequency range from 3.1 GHz to 10.6 GHz for commercial purposes and FCC limited the power spectral density emission for UWB to -41.3 dBm/MHz. In 2007, UK regulator Office of Communications (OFCOM) announced a similar policy. There has been a great concern over interference between various narrowband signals and UWB signals that share the same frequency spectrum, such as WLAN in the frequency band centered at 5.8 GHz.

## 2.4 Simplified Composite Right/Left Handed (SCRLH) Resonator

In early 2004, Sanada designed a general composite right/left-handed (CRLH) transmission line resonator structure [24], whose schematic circuit is shown in Figure 2.4. The difference between right handed and left handed transmission lines is the inductors and capacitors are connected in an opposite position. Figure 2.4 shows a combined LH and RH unit [26].

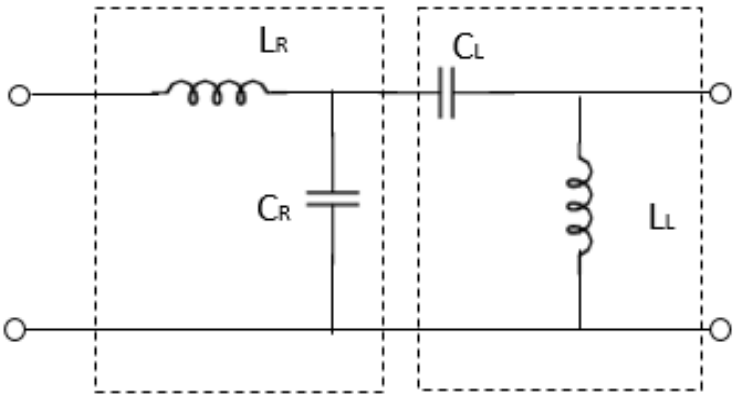


Figure 2.4 Combined LH and RH unit [26].

Later-in 2006, Lin introduced a simplified CRLH (SCRLH) transmission line with no equilibrium condition [11]. Both the structure size and complexity of the CRLH are reduced by removing the series capacitor or shunt inductor.

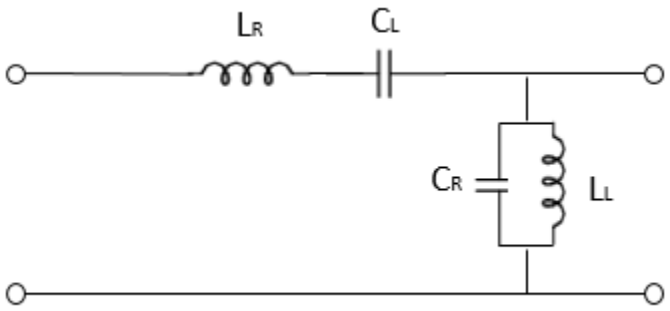


Figure 2.5 Schematic circuit of a CRLH unit [26].

According to references [10], [21] and [25], an SCRLH resonator has an inherent dual-mode property, in which the two resonant frequencies of the SCRLH resonator can be evaluated as follows [26]:

$$f_1 = \left(\frac{1}{L_L \times C_R}\right)^{1/2} \tag{2.4}$$

$$f_2 = \left(1 + \frac{4L_L}{L_R}\right)^{1/2} / (L_L \times C_R)^{1/2} \tag{2.5}$$

where $L_R$ is the series inductance, $C_R$ is the shunt capacitance and $L_L$ is the shunt inductance.

The dispersion relation and characteristic impedance of a SCRLH resonator can be obtained by using Bloch-Floquet theory as shown below [27]:

$$\beta(\omega)d = \cos^{-1}\left(1 + \frac{ZY}{2}\right) \tag{2.6}$$

$$ZB = \frac{\sqrt{\left(\frac{ZY}{2}\right)^2 + ZY}}{Y} \tag{2.7}$$

where $\beta$ is the propagation constant for Bloch waves, *ZB* and *d* are, respectively, the characteristic impedance and the length of the unit cell of the SCRLH resonator. The series impedance and shunt admittance can be evaluated by [27]:

$$Z(\omega) = j\omega L_R \tag{2.8}$$

$$Y(\omega) = \frac{1 - \omega^2 C_R L_L}{j\omega L_L} \tag{2.9}$$

As a brief summary, this chapter has mainly discussed the basic concepts and terminologies used in UWB-BPF analysis and design, which has served as the background preparation for successfully building a new ellipse-shaped UWB-BPF with a notched band.

# CHAPTER 3 DESIGN OF SCRLH UWB-BPF

In this work, the main objective is to design a highly compact ellipse-shaped ultra-wideband bandpass filter (UWB-BPF) by superposing two cross-shaped microstrip line segments and a defected ground structure (DGS) onto an ellipse-shaped ring with two ground vias. When designing this UWB-BPF, the first step is to design an ellipse-shaped simplified composite right/left handed (SCRLH) BPF which will be discussed in this chapter. The S-parameter characteristics and some potential issues will also be included in this chapter. While to accomplish the desired notched band, the second step of UWB-BPF design will be integrating two curved open stepped-impedance (SI) stubs and DGS to the designed UWB-BPF which will be discussed later in the next chapter.

## 3.1 Design of SCRLH UWB-BPF

The SCRLH transmission line structure was firstly studied in [11]. The SCRLH resonator is made up of high/low-impedance short-line and grounded stub with metalized via hole [10], [27]. In this work, a novel SCRLH UWB-BPF is designed with two important parts. As shown below in Figure.3.1, the first part is an ellipse-shaped ring with two ground vias centered at the top and bottom sides of the ring. The second part is a pair

of cross-shaped microstrip line segments in the middle of the ring in order to reduce the return loss in the passband. The dimensions of the structure in Figure 3.1 are summarized as follows: $L_1 = 3.48$, $L_2 = 12.59$, $L_3 = 2.92$, $L_4 = 2.24$, $W_1 = 0.15$, $W_2 = 0.4$, $W_3 = 1.35$ all in mm. The radiuses of both vias are 0.2mm. The substrate used in the designed SCRLH UWB-BPF is FR4 with relative permittivity of 4.4, loss tangent of 0.02 and thickness of 0.7mm. All the metals used in this design are copper with thickness of 35 µm and conductivity of $5.8 \times 10^7$ S/m.

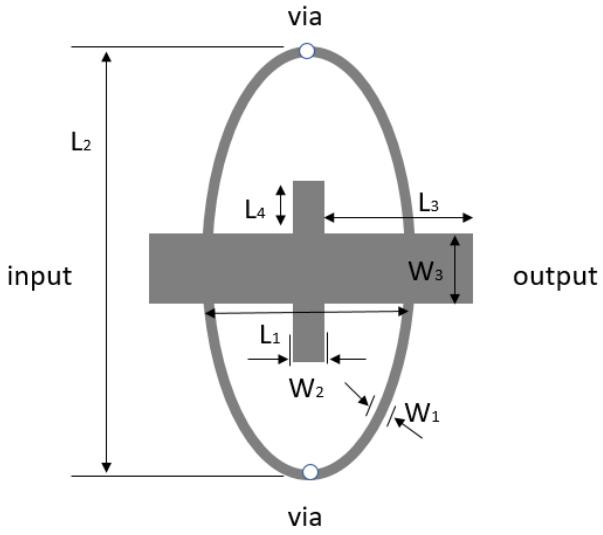


Figure.3.1 Geometry of the SCRLH UWB-BPF.

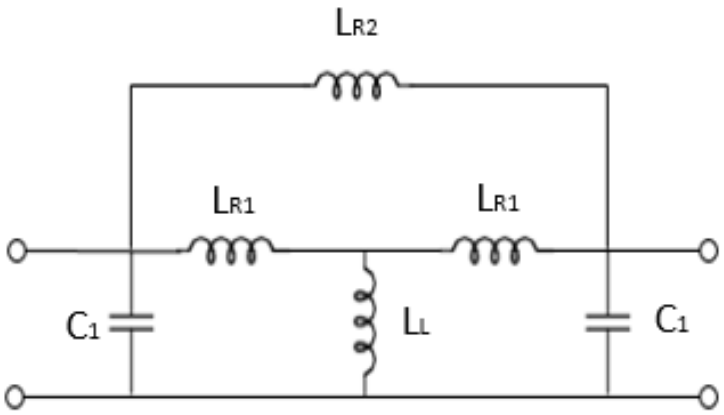


Figure 3.2 Schematic circuit of the SCRLH UWB-BPF.

Figure.3.1 shows the top view of the proposed SCRLH UWB-BPF and Figure 3.2 represents its corresponding equivalent schematic circuit. As seen in Figure 3.2, $L_L$ represents the left-handed shunt inductance measured at two vias, $L_{R1}$ and $C_1$ stands for the right-handed series inductance and shunt capacitance induced by the ellipse-shaped ring, and $L_{R2}$ is inductance determined by the cross-shaped microstrip line segments.

## 3.2 S-Parameter Analysis and Potential Issues

Figure 3.3 shows the High Frequency Electromagnetic Field Simulation (HFSS) simulated S-parameters of the designed UWB-BPF without the cross-ellipse-shaped DGS and the two open SI stubs.

As shown in Figure 3.3, the 3dB passband ranges from 2.94 GHz to 12.83 GHz, which has shown a potential to provide a very broadband characteristic in UWB communication.

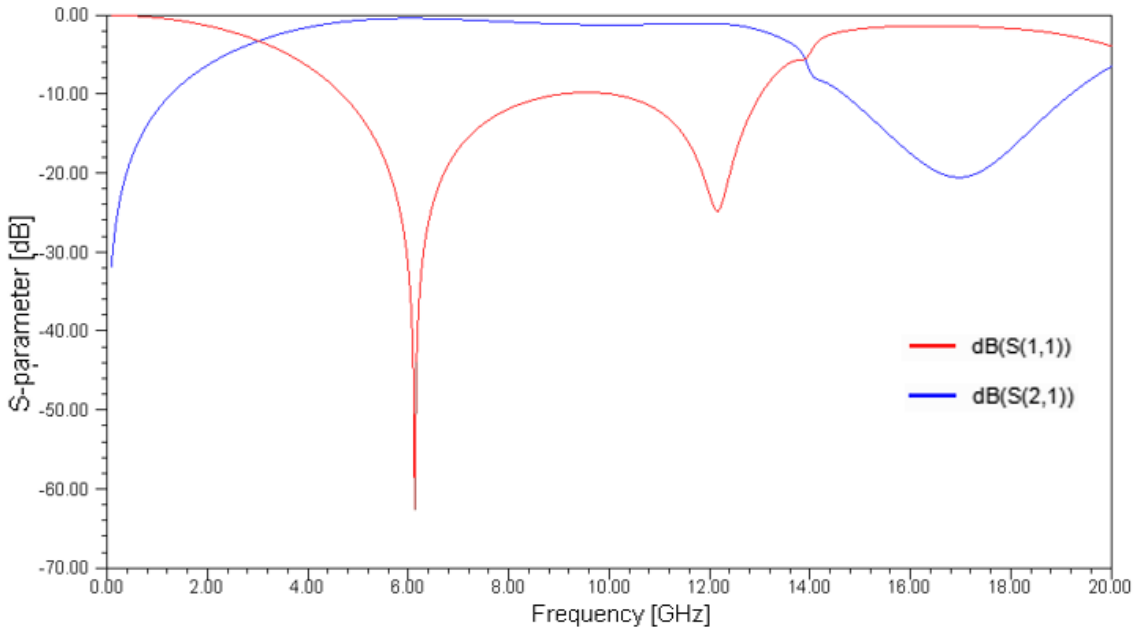


Figure 3.3 Simulated S-parameters of UWB-BPF without cross-ellipse-shaped DGS and two open SI stubs.

However, one of the objective of this research is to reject unwanted interference signals from WLAN applications in the frequency neighborhood of 5.8 GHz. The current UWB-BPF will not be able to reject WLAN noise as observed in Figure 3.3. Thus, a notched band needs to be added to this UWB-BPF configuration to meet the design objectives, which will be further developed in the next chapter.

# CHAPTER 4 DESIGN OF THE UWB-BPF WITH A NOTCHED BAND

In this chapter, a notched band will be added to the UWB-BPF designed in the previous chapter in order to reject unwanted WLAN interference signals in the frequency range of 5.8 GHz. The proposed notched band is achieved by integrating two open, curved stepped-impedance stubs and a cross-ellipse-shaped defected ground structure (DGS) to the designed UWB-BPF.

## 4.1 Integration of Two SI Stubs and a DGS to the Designed UWB-BPF

A desired notched band has been achieved by connecting two open Stepped-Impedance (SI) stubs and a cross-ellipse-shaped defected ground structure (DGS) to the designed UWB-BPF as shown below in Figure.4.1.

The finally tuned dimensions of the structure are characterized with $L_5 = 2.5$, $L_6 = 3.58$, $L_7 = 0.63$, $W_4 = 0.66$, $W_5 = 0.16$, $W_6 = 1.5$, $W_7 = 3$, $W_8 = 2.4$, $W_9 = 4$, $W_{gap} = 0.44$ all in mm. The substrate and metals used in this design are identical to those mentioned in chapter 3. Namely, the substrate used in the designed structure is FR4 with relative permittivity of 4.4, loss tangent of 0.02 and thickness of 0.7mm, and all the metals used in this design are copper with thickness of 35 μm and conductivity of $5.8 \times 10^7$ S/m.

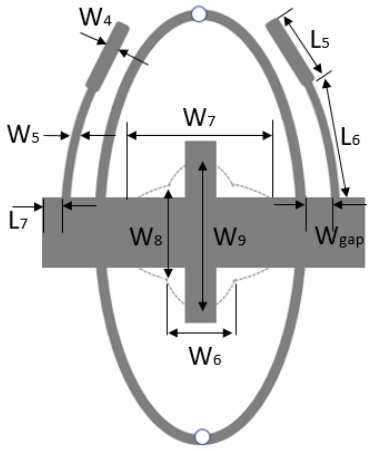


Figure 4.1 Geometry of the designed UWB-BPF with two open SI stubs and DGS.

The equivalent schematic circuit of the UWB-BPF with two open SI stubs and DGS is shown below in Figure 4.2, which can be used to systematically assess the proposed enhanced version of the UWB-BPF.

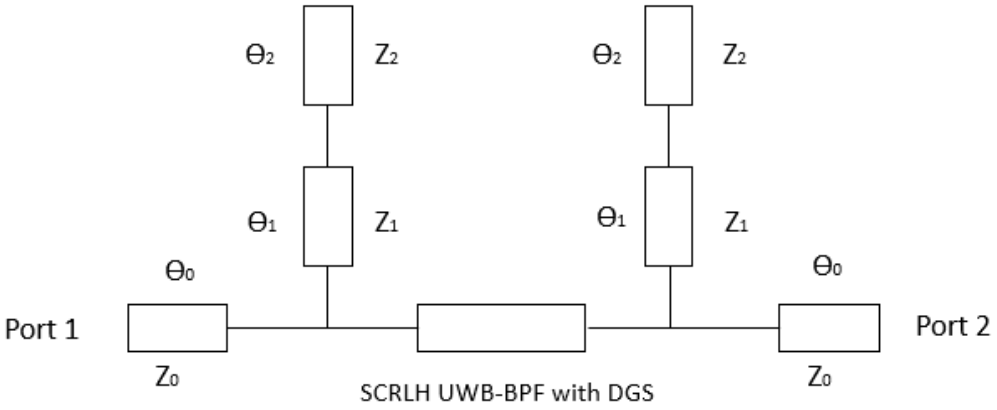


Figure 4.2 Equivalent schematic circuit of the UWB-BPF with two open SI stubs and DGS.

In Figure 4.2, $Z_0$ represents the characteristic impedances of the matched input and output transmission lines, $Z_1$ and $Z_2$ are the characteristic impedances of the two SI stubs, $\Theta_0$ is the electrical length of the transmission line with $Z_0$, while $\Theta_1$ and $\Theta_2$ are the electrical lengths of the transmission lines with $Z_1$ and $Z_2$. The following expressions show the admittances of the two open SI stubs [8]:

$$Y_{SI} = Y_1 = Y_2 \tag{4.1}$$

$$Y_{SI} = \frac{j}{Z_1}\left(\frac{Z_1 + Z_2 \tan\theta_1 \cot\theta_2}{Z_2 \cot\theta_2 - Z_1 \tan\theta_1}\right) \tag{4.2}$$

where $Y_1$ and $Y_2$ represents the total admittance of each SI stub [8].

## 4.2 S-Parameter Analysis of the UWB-BPF

Figure 4.3 represents the HFSS simulated S-parameters of the UWB-BPF with the DGS and two open SI stubs.

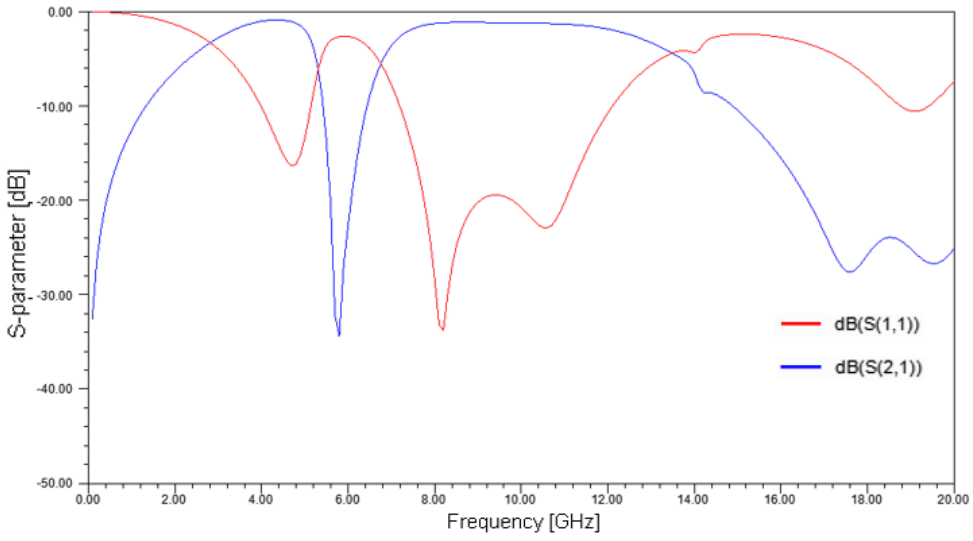


Figure 4.3 Simulated S-parameters of the UWB-BPF with DGS and two open SI stubs.

As shown in Figure 4.3, the original passband has been split to two passbands ranging from 2.94 through 5.14 GHz and 7.12 through 12.83 GHz, respectively, due to adding the proposed notched band. The notched band reaches to about 35 dB maximum attenuation with about 2 GHz bandwidth centered at 5.8 GHz frequency, which is measured at the return loss of -10dB. The design has successfully met one of the objectives, which is to reject the unwanted WLAN interference signals in the frequency range of 5.8 GHz. It is found that the return loss in the passband is quite sensitive to the variation of $W_5$ [8] and the finalized $W_5$ is set to be 0.16mm. The total dimension is about 14mm × 6.2mm which is slightly smaller than that presented in [8].

Group delay is a measure of signal distortion which indicates the actual transit time of the signal through the designed UWB-BPF as a function of frequency, which is precisely defined as the following [8]:

$$Group\ Delay = \frac{-d\varphi}{d\omega} = \frac{-1}{360^\circ} \cdot \frac{d\theta}{df} \tag{4.3}$$

$$\omega = 2\pi f \tag{4.4}$$

where dφ and dω are the differential phase and frequency changes.

Figure 4.4 shows that the predicted group delay is mostly very flat in the range of 0.1 to 0.3 ns within the passbands, which is highly desirable because the variations in the group delay can cause signal distortion. It is found that the group delay peaks in the neighborhood of 5.8 GHz within the notched band region, which will not essentially affect the output signals.

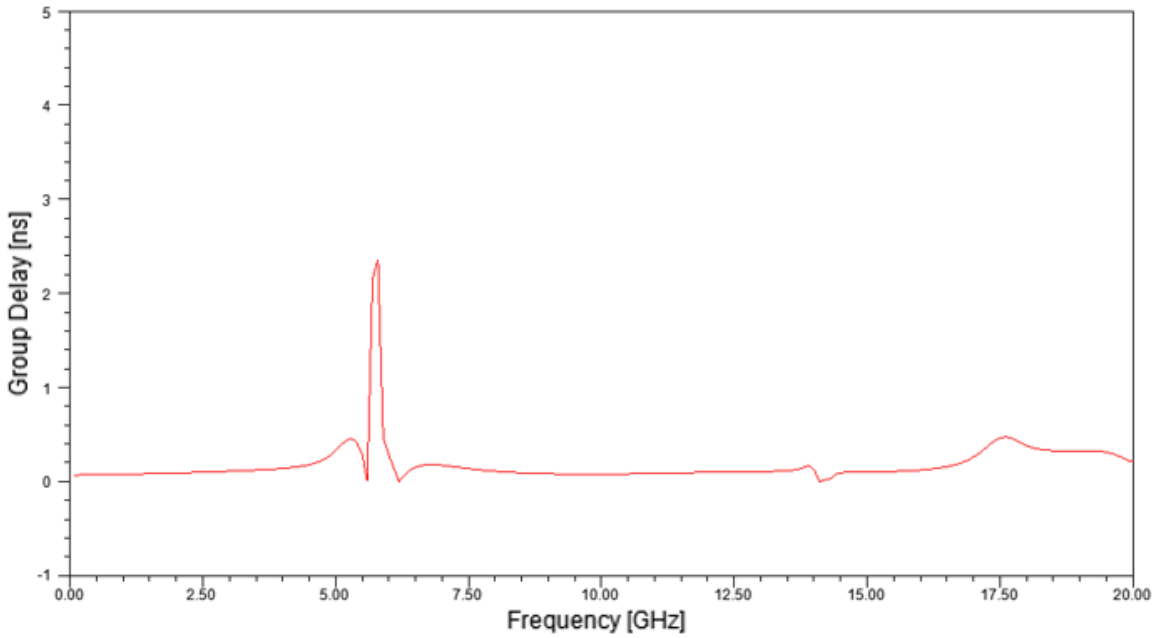


Figure 4.4 Group delay of the designed UWB-BPF.

Apparently, the designed UWB-BPF will be able to successfully reject undesired WLAN interference signals in the 5.8 GHz frequency band while allowing other frequencies to pass with minimum loss with a really small group delay.

As the summary of the chapter, two open SI stubs and a cross-ellipse-shaped DGS have been integrated to the UWB-BPF designed in chapter 3 to further improve the characteristics of the UWB-BPF and to achieve a highly attenuated notched band in the frequency neighborhood of 5.8 GHz.

# CHAPTER 5 ANALYSIS, MODELING AND VALIDATION OF THE UWB-BPF SYSTEM

This chapter will focus on the analysis method for the blocked UWB-BPF system, the HFSS modeling of the structure, and the validation of the designed UWB-BPF design. In addition, some recently published UWB-BPFs will be used for comparison.

## 5.1 UWB-BPF System ABCD Matrix

In order to systematically evaluate the UWB-BPF shown in Figure 4.1, the proposed UWB-BPF circuit has been divided into five parts as shown in Figure 5.1: the SCRLH UWB-BPF with the DGS (Part 1), two open SI stubs (Part 2 and Part 3), input transmission line (Part 4) and output transmission line (Part 5).

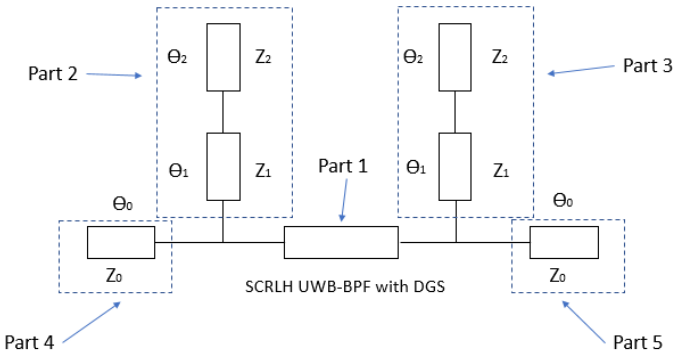


Figure 5.1 Five parts of the designed UWB-BPF

Thus, the total ABCD matrix of the designed UWB-BPF system can be systematically derived from each part transmission matrix as shown in equation (5.1).

$$\begin{bmatrix} A & B \\ C & D \end{bmatrix} = \begin{bmatrix} A_1 & B_1 \\ C_1 & D_1 \end{bmatrix} \begin{bmatrix} 1 & 0 \\ Y_1 & 1 \end{bmatrix} \begin{bmatrix} A_2 & B_2 \\ C_2 & D_2 \end{bmatrix} \begin{bmatrix} A_1 & B_1 \\ C_1 & D_1 \end{bmatrix} \begin{bmatrix} 1 & 0 \\ Y_2 & 1 \end{bmatrix} \quad (5.1)$$

where $Y_1$ and $Y_2$ are evaluated by equations (5.2) and (5.3), namely, equation (4.1) and (4.2).

$$Y_{SI} = Y_1 = Y_2 \quad (5.2)$$

$$Y_{SI} = \frac{j}{Z_1}\left(\frac{Z_1 + Z_2 \tan\theta_1 \cot\theta_2}{Z_2 \cot\theta_2 - Z_1 \tan\theta_1}\right) \quad (5.3)$$

$A_1B_1C_1D_1$ stands for the transmission matrix of the input and output lines (Part 4 and Part 5), $A_2B_2C_2D_2$ represents the transmission matrix of the SCRLH UWB-BPF with the DGS structure (Part 1) [8], which can be deduced by the equivalent circuit in Figure 3.2 and Figure 5.1.

The $A_1B_1C_1D_1$ matrix is given as:

$$\begin{bmatrix} A_1 & B_1 \\ C_1 & D_1 \end{bmatrix} = \begin{bmatrix} \cos\theta_0 & jZ_0 \sin\theta_0 \\ j/Z_0 \sin\theta_0 & \cos\theta_0 \end{bmatrix} \quad (5.4)$$

where $Z_0$ represents the characteristic impedances of the matched input and output transmission lines, $Z_1$ and $Z_2$ are the characteristic impedances of the two SI stubs, $\Theta_0$ is the electrical length of the transmission line with $Z_0$, while $\Theta_1$ and $\Theta_2$ are the electrical lengths of the transmission lines with $Z_1$ and $Z_2$.

## 5.2 High Frequency Electromagnetic Field Simulation

High Frequency Electromagnetic Field Simulation (HFSS) is a software that commonly used in the industry for 3D full-wave electromagnetic fields simulation using the finite element method [29]. It was originally developed by Prof. Zontal Cendes and his students at Carnegie Mellon University in 1989. It has been widely used for various analysis and design of electromagnetic applications, such as antennas, passive RF components, connectors and PCBs. By using HFSS, engineers and researchers can design different applications and study the device characteristics with lower design costs and smaller design cycles.

In this work, HFSS was used to design the entire UWB-BPF structure, including the UWB-BPF, SI stubs, and ellipse-shaped cross DGS. Figures 5.2 and 5.3 have shown the developed HFSS design for the original UWB-BPF and its improved version with two open SI stubs and the DGS ground structure.

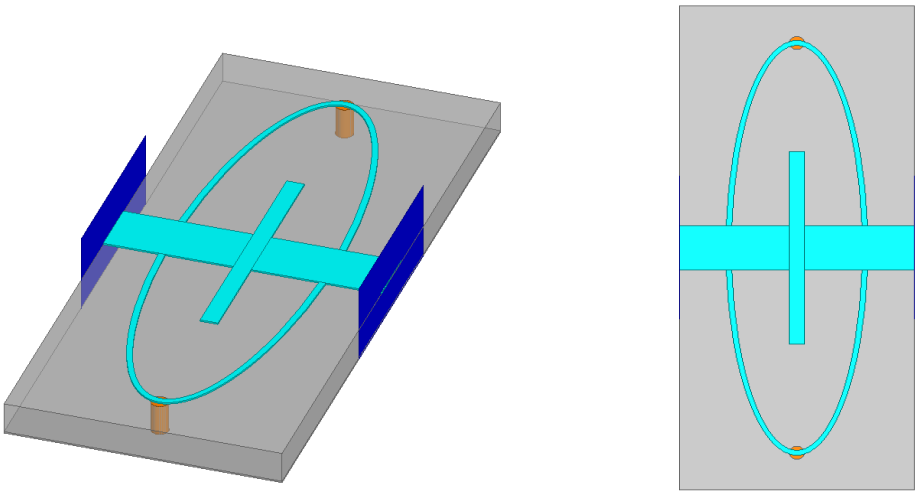

Figure 5.2 HFSS designed UWB-BPF.

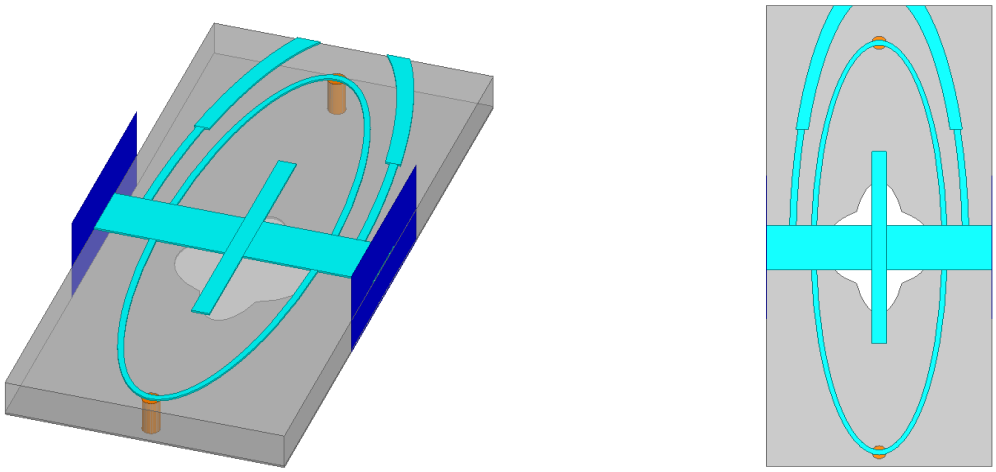

Figure 5.3 HFSS designed UWB-BPF with two open SI stubs and DGS.

Both the models, as shown in Figures 5.2 and 5.3, have provided a clear view of the designed UWB-BPF geometries, which was exceedingly helpful in finding accurate simulation results.

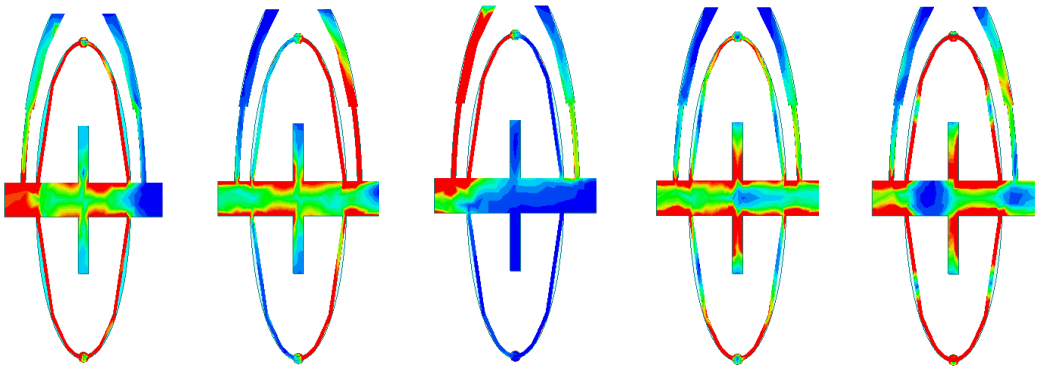

(a) (b) (c) (d) (e)

Figure 5.4 HFSS current density distribution for the designed UWB-BPF at different frequencies, (a) 0.8GHz, (b) 4.1 GHz, (c) 5.8 GHz, (d) 10 GHz, (e) 13.5 GHz.

Figure 5.4 shows the simulated current density images distributed on the surface of the metal layer for the enhanced UWB-BPF. It is found that at frequencies of 4.1 GHz and 10 GHz within the passband, the current mainly distributes on both the ellipse-shaped ring and the cross-shaped microstrip line segments from the input port to the output port as shown in 5.4 (b) and 5.4 (d). For 0.8 GHz and 13.5 GHz frequency points within the lower frequency stopband and higher frequency stopband, however, the currents are not able to flow to the output port as demonstrated in 5.4 (a) and 5.4 (e). At frequency of 5.8 GHz located in the notched band, the current signals are mostly blocked at the open SI stub near the input port as shown in 5.4 (c).

The current density distribution images of the five sample frequencies clearly indicate that the designed UWB-BPF successfully rejected the unwanted WLAN interference signals in the frequency range of 5.8 GHz while allowing other frequencies to pass with minimum loss.

## 5.3 Validation of UWB-BPF

Since the fabrication of the designed UWB-BPF has not been included in this research, the design approach and accuracy have been validated by using a rectangular-shaped UWB-BPF as documented in [8]. In [8], a rectangular-shaped UWB-BPF was designed by Yang and his group, where the S-parameters are simulated and measured as shown below in Figure 5.5.

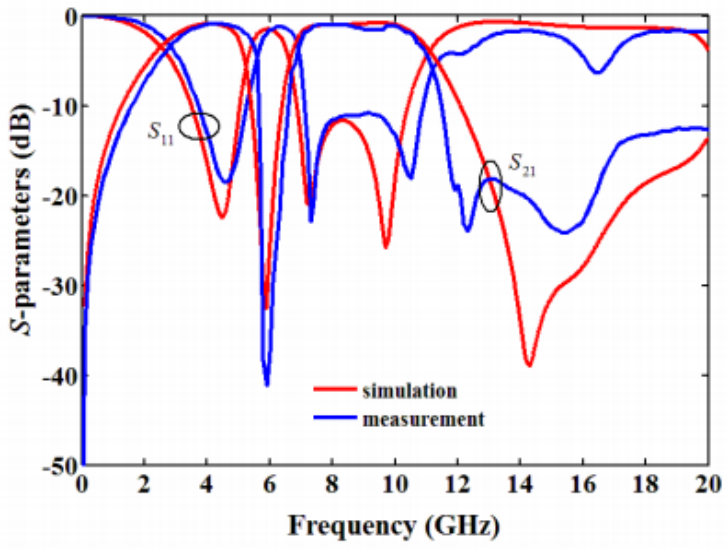


Figure 5.5 Simulated and measured S-parameters for a square-shaped UWB-BPF [8].

By using the provided geometry dimensions and substrate, a similar simulation was done to verify the results and the simulated S-parameters results are achieved in Figure 5.6.

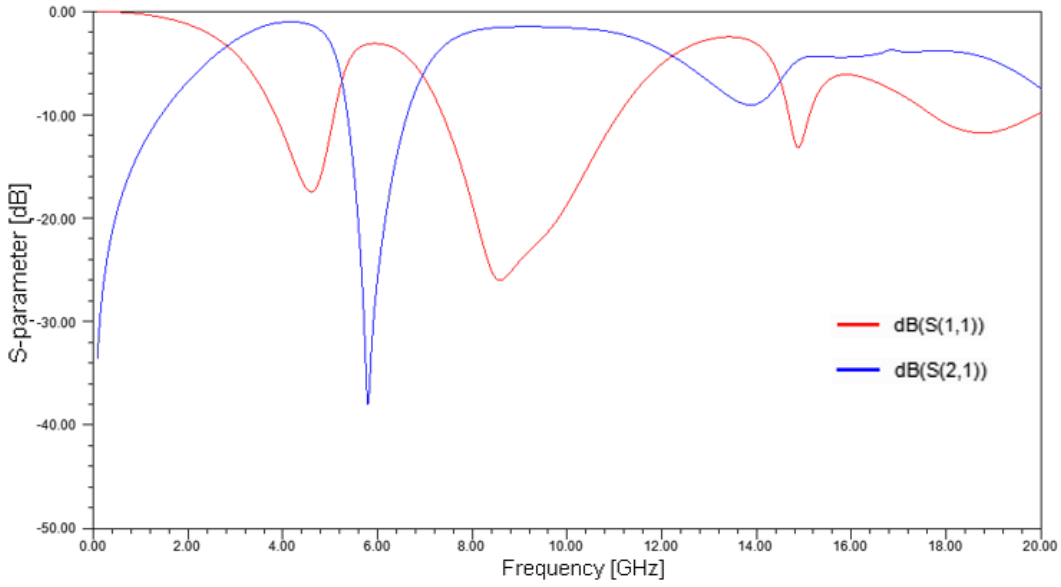


Figure 5.6 Simulated S-parameters for design in [8].

It is observed that a fairly consistent result has been achieved by comparing these two designs with small shifts at the edges of the two passbands. Namely, in Figure 5.5, the two 3dB passbands ranges, respectively, from 3.05 to 5.39 and 6.25 to 10.67 GHz, while in this design as shown in Figure 5.6, the two 3dB passbands ranges, respectively, from 3.0 to 5.15 and 7.0 to 11.14 GHz. The deference between this work and that documented in [8] may be resulted from dimension and material information for Yang's UWB-BPF, which causes some small shifts at the edges of the two passbands.

## 5.4 Characteristic Comparison to Published Designs

It has been observed that most published UWB-BPF designs usually require a very complicated geometry and large dimensions to achieve satisfied performance in the passband and notched band. Apparently, the total dimension of the designed UWB-BPF in this work is the smallest in comparison to those recently published ones [3,8,9,10] as summarized below in Table 5.1.

Table 5.1 Comparison with recently published UWB-BPF designs.

| Reference | Substrate Thickness (mm) | $\varepsilon_r$ | Notched Band Center Frequency (GHz) | Attenuation (dB) | Structure Size (mm) |
|---|---|---|---|---|---|
| [3] | 0.635 | 6.15 | 5.41 | 11 | 9.62 × 16.7 |
| [8] | 0.7 | 4.4 | 5.82 | 40 | 6.2 × 14.1 |
| [9] | 0.787 | 2.2 | 5.83 | 18 | 4.2 × 23.26 |
| [10] | 1.0 | 2.2 | 5.85 and 8.0 | 15 | 20 × 34 |
| This design | 0.7 | 4.4 | 5.80 | 35 | 6.2 × 14.0 |

As shown above in Table 5.1, the designed UWB-BPF in this work has the smallest structure size in comparison to those sizes in [3], [8], [9] and [10] while keeping a decent attenuation with the minimum of -35 dB.

# CHAPTER 6 CONCLUSION AND FUTURE WORK

## 6.1 Conclusion

In this work, an enhanced UWB-BPF with a pair of cross-ellipse-shaped DGS and two open SI stubs has been properly designed. The design has achieved a good passband with a notched band of 35 dB maximum attenuation in the frequency neighborhood of 5.80 GHz. Also, it is found that the phase distortion of the designed UWB-BPF is negligible since a very flat group delay response is detected within the desired passbands.

This UWB-BPF has a very competitive overall structure size and provides a great S-parameter performance. In practice, the frequency band of the notch filter can be easily adjusted by simply changing or tuning $L_5$ and $L_6$ to meet different applications.

As a conclusion, the designed ellipse-shaped UWB-BPF can be potentially applied to UWB systems considering its compact structure size, low-profile geometry, and great S-parameter performance.

## 6.2 Future Work

In future work, the proposed UWB-BPF can be certainly further improved and enhanced by considering the following research:

- Implement different practical PCBs in future UWB-BPF design and enhancement with various relative permittivity and thickness values. For example, use a multi-layer PCB to add flexibility to UWB-BPF design to vary inductance and capacitance, to route circuit paths, and to add more vias;
- Change the frequency location of the notched band by tuning and optimizing the UWB-BPF geometry parameters to meet different application requirements. Or even add multiple notched bands to the UWB-BPF simultaneously and to reject interference signals in different frequencies;
- Reduce the bandwidth of the notched band to improve the passband width. It can be potentially decreased by improving the quality factors of the SCRLH resonator. For instance, adding more vias, changing the circuit pattern, or adopting different schematic circuit topologies.

# REFERENCES


[1] H. Shaman and J.-S. Hong, "Ultra-wideband (UWB) bandpass filter with embedded band notch structures," *IEEE Microw. Wireless Compon. Lett.*, pp. 193–195, vol. 17, no. 3, Mar. 2007.

[2] S. W. Wong and L. Zhu, "Implementation of compact UWB bandpass filter with a notch-band," *IEEE Microw. Wireless Compon. Lett.*, pp. 10–12, vol. 18, no. 1, Jan. 2008.

[3] C. H. Kim and K. Chang, "Ring resonator bandpass filter with switchable bandwidth using stepped-impedance stubs," *IEEE Trans. Microw. Theory Tech.*, pp. 3936–3944, vol. 58, no. 12, Dec. 2010.

[4] Z.-C. Hao, J.-S. Hong, J. P. Parry, and D. P. Hand, "Ultra-wideband bandpass filter with multiple notch bands using nonuniform periodical slotted ground structure," *IEEE Trans. Microw. Theory Tech.*, pp. 3080–3088, vol. 57, no. 12, Dec. 2009.

[5] G.-M. Yang, R. Jin, C. Vittoria, V. G. Harris, and N. X. Sun, "Small ultra-wideband (UWB) bandpass filter with notched band," *IEEE Microw. Wireless Compon. Lett.*, pp. 176–178, vol. 18, no. 3, Mar. 2008.

[6] K. Chang, ***Microwave Ring Circuits and Antennas***. New York: Wiley, 1996, ch. 2.

[7] R. Li and L. Zhu, "Compact UWB bandpass filter using stub-loaded multiple-mode resonator," *IEEE Microw. Wireless Compon. Lett.*, pp. 40–42, vol. 17, no. 1, Jan. 2007.

[8] S. Yang, Y. Chen, G. Lu, L Wang, B. Li and D. Zeng, "Design of a highly compact UWB-BPF with a notched band using a SCRLH resonator and two open SI stubs," submitted to *IEEE Microw. Wireless Compon. Lett.*

[9] J. Li, C. Ding, F. Wei, and X. W. Shi, "Compact UWB BPF with notch band based on SW-HMSIW," *Electron. Lett.*, pp. 1338-1339, vol. 51, no. 17, 2015.

[10] F. Wei, Q.Y. Wu, X.W. Shi, and L. Chen, "Compact UWB bandpass filter with dual notched bands based on SCRLH resonator," *IEEE Microw. Wirel. Compon. Lett.*, pp. 28-30, vol. 21, no. 1, 2011.

[11] X. Q. Lin, R. P. Liu, and X. M. Yang, "Arbitrary dual-band components using simplified structures of conventional CRLH TLs*," IEEE Trans. Microw. Theory Tech.*, pp. 2902–2909, vol. 54, no. 7, Jul. 2006.

[12] S.Y. Huang and Y.H. Lee, "Development of Ultra-wideband (UWB) Filters," Nanyang Technological University.

[13] J. Hong and M. J. Lancaster, "Couplings of microstrip square open-loop resonators for cross-coupled planar microwave filters," *IEEE Trans. Microw. Theory Tech.*, vol. 44, no. 11, Nov. 1996.

[14] J. Kuo, T. Yeh and C. Yeh, "Design of microstrip bandpass filters with a dual-passband response," *IEEE Trans. Microw. Theory Tech.*, vol. 53, no. 4, Apr. 2005.

[15] H. Wang, L. Zhu and W. Menzel, "Ultra-wideband bandpass filter with hybrid microstrip/CPW structure," *IEEE Microwave and Wireless Components Letters.* vol. 15, no. 12, Dec. 2005.

[16] J. Bonache, I. Gil, J. Garcia-Garcia and F. Martin, "Novel microstrip bandpass filters based on complementary split-ring resonators," *IEEE Trans. Microw. Theory Tech.*, vol. 54, no. 1, Jan. 2006.

[17] L. Hsieh and K. Chang, "Compact, low insertion-loss, sharp-rejection, and wide-band microstrip bandpass filters," *IEEE Trans. Microw. Theory Tech., vol.* 51, no. 4, Apr. 2003.

[18] S. Sun and L. Zhu, "Compact dual-band microstrip bandpass filter without external feeds," *IEEE Microwave and Wireless Components Letters.* vol. 15, no. 10, Oct. 2005.

[19] C. Chen and C. Hsu, "A simple and effective method for microstrip dual-band filters design," *IEEE Microwave and Wireless Components Letters.* vol. 16, no. 5, May. 2006.

[20] J. T. Kuo and E. Shih, "Microstrip stepped impedance resonator bandpass filter with an extended optimal rejection bandwidth," *IEEE Trans. Microw. Theory Tech.*, vol. 51, no. 5, May. 2003.

[21] W. Han and Y. Feng, "Ultra-wideband bandpass filter using simplified left-handed transmission line structure," *Microwave and Optical Technology Letters*, pp. 2758-2762, vol. 50, no. 11, 2008.

[22] *Basic Electronics Tutorials*. "Band Pass Filter - Passive RC Filter Tutorial," electronics-tutorials.ws, Nov. 2016. Accessed 13. June 2017.

[23] *Basic Electronics Tutorials*. "Band-Stop Filter" electronics-tutorial.ws, Nov. 2016. Accessed 21 June 2017.

[24] A. Sanada, C. Caloz, and T. Itoh, "Characteristics of the composite right/left-handed transmission lines," *IEEE Microwave and Optical Technology Letters*, vol. 14, no. 2, February 2004.

[25] X. Yang, L. Lin, G. Liu and W. Cheng, "Signal interference between CRLH TL and RH TL," *Electronics Letters*, pp.1236-1238, vol. 52, no. 14, July 7th, 2016.

[26] C. Caloz and T. Itoh, ***Electromagnetic Metamaterials: Transmission Line Theory and Microwave Applications***. *Wiley-Interscience*. 2006. pp.16-17.

[27] J.K. Wang and Y.J. Zhao, "A miniaturized UWB BPF based on novel SCRLH transmission line structure," *Electromagnetics Research Letters*, pp.67-73, vol.19, 2010.

[28] S. Khan and J. L. Mauri, ***Green Networking and Communications: ICT for Sustainability***. *Taylor & Francis Group, LLC*. 2014. p347, p211.

[29] M. Long, ***World Congress on Medical Physics and Biomedical Engineering***. *IFMBE Proceedings*, pp51, vol. 39 May 2012.